

## How to Detect Internal Motion by Homonuclear NMR

Jürgen Schleucher\* and Sybren S. Wijmenga\*

Contribution from the Department of Medical Biochemistry and Biophysics, and  
Department of Organic Chemistry, Umeå University, S-90187 Umeå, Sweden

Received August 24, 2001. Revised Manuscript Received February 1, 2002

**Abstract:** NOESY and ROESY cross-peak intensities depend on internuclear distances and internal motion. Internal motion is usually ignored, and NOESY cross-peak intensities are interpreted in terms of internuclear distances only. Off-resonance ROESY experiments measure a weighted average of NOE and ROE. The weight can be described and experimentally set by an angle  $\theta$ . For large enough molecules, NOE and ROE have opposite signs. Therefore, each cross-peak intensity becomes zero for an angle  $\theta^0$ . For any sample, the maximum angle  $\theta^0$  is determined by the overall motion of the molecule. Smaller  $\theta^0$  values reflect the angular component of internal motions. Because individual cross-peaks are analyzed, the method evaluates internal motions of individual H,H vectors. The reduction of  $\theta^0$  is largest for internal motions on a time scale of 100–300 ps. The sensitivity of  $\theta^0$  for internal motions decreases with increasing molecular weight. We estimate that detecting internal motions will be practicable for molecules up to about 15 kDa. We describe a protocol to measure  $\theta^0$  from a series of off-resonance ROESY spectra. For such a series, we describe the choice of experimental parameters, a procedure to extract  $\theta^0$  from the raw data, and the interpretation of  $\theta^0$  in terms of internal motions. In the small protein BPTI, we analyzed 75 cross-peaks. The precision of  $\theta^0$  was 0.25°, as compared to typical reductions of  $\theta^0$  of 3°. We found a well-defined maximum  $\theta^0$  for cross-peaks in rigid parts of the molecule, which reflects the overall motion of the molecule. For BPTI, also many structurally important long-range cross-peaks appear rigid. The lower  $\theta^0$  values of long-range contacts involving methyl groups are consistent with methyl rotation on the 25-ps time scale. The lower  $\theta^0$  values of the flexible C-terminus and of flexible side chains translate into upper limits for the angular order parameter of 0.4 and 0.5–0.8, respectively. Off-resonance ROESY can monitor internal motions of H,H contacts that are used in a structure calculation. Because no isotope labeling is needed, off-resonance ROESY can be used to detect internal motions in a wide range of natural products.

### Introduction

Biomacromolecules show internal motions on an enormous range of time scales from picoseconds to seconds.<sup>1</sup> Internal motions are required for the biological function of all classes of biomacromolecules: Proteins must be flexible for induced-fit binding.<sup>2</sup> Nucleic acids need flexibility for molecular recognition, such as in the formation of the U1A–RNA complex.<sup>3</sup> Free oligosaccharides can exist in single or multiple conformations, with internal motions on a wide range of time scales.<sup>4–6</sup> Oligosaccharides can bind to proteins with or without conformational change.<sup>7,8</sup> For glycoproteins, very little is known about the motions between the sugar and protein part.<sup>9</sup> In

general, it remains a challenge to link internal motions of free biomacromolecules to function. Therefore, methods are needed to assess internal motions of biomacromolecules.

NMR is beginning to map the changes in internal motions associated with biological function,<sup>10–13</sup> using experiments designed to monitor internal motions. Internal motions affect NMR spectra of biomacromolecules, via their influence on relaxation of nuclear spins in NMR experiments. Relaxation describes how fast NMR signals decay, or how fast signals recover from being perturbed in NMR experiments. The most common experiments study the relaxation of the heteronuclei <sup>15</sup>N, <sup>13</sup>C, or <sup>2</sup>H.<sup>14–16</sup> These heteronuclear relaxation experiments have usually been applied to isotope-labeled samples. Because <sup>15</sup>N labeling of proteins is most affordable, protein backbone motions have been studied most frequently. Isotope labeling of

\* To whom correspondence should be addressed. J.S.: E-mail, jurgen@rabbit.chem.umu.se; phone, +46-90-786-5388. S.S.W.: E-mail, sybren@indigo.chem.umu.se; phone, +46-90-786-6080; fax, +46-90-136310.

- (1) McCammon, J. A.; Harvey, S. C. *Dynamics of Proteins and Nucleic Acids*; Cambridge University Press: Cambridge, 1987.
- (2) Creighton, T. E. *Proteins: Structures and Molecular Properties*; W. H. Freeman & Co.: New York, 1993.
- (3) Varani, G. *Acc. Chem. Res.* **1997**, *30*, 189–195.
- (4) Rutherford, T. J.; Homans, S. W. *Biochemistry* **1994**, *33*, 9606–9614.
- (5) Peters, T.; Pinto, B. M. *Curr. Opin. Struct. Biol.* **1996**, *6*, 710–720.
- (6) Bush, C. A.; Martin-Pastor, M.; Imberty, A. *Annu. Rev. Biophys. Biomol. Struct.* **1999**, *28*, 269–293.
- (7) Poppe, L.; Brown, G. S.; Philo, J. S.; Nikrad, P. V.; Shah, B. H. *J. Am. Chem. Soc.* **1997**, *119*, 1727–1736.
- (8) Poveda, A.; Jiménez-Barbero, J. *Chem. Soc. Rev.* **1998**, *27*, 133–143.

- (9) Erbel, P. J. A.; Karimi-Nejad, Y.; van Kuik, J. A.; Boelens, R.; Kamerling, J. P.; Vliegthart, J. F. G. *Biochemistry* **2000**, *39*, 6012–6021.
- (10) Kay, L. E.; Muhandiram, D. R.; Wolf, G.; Shoelson, S. E.; Forman-Kay, J. D. *Nat. Struct. Biol.* **1998**, *5*, 156–163.
- (11) Palmer, A. G. *Curr. Opin. Struct. Biol.* **1997**, *7*, 732–737.
- (12) Feher, V. A.; Cavanagh, J. *Nature* **1999**, *400*, 289–293.
- (13) Lee, A. L.; Kinnear, S. A.; Wand, A. J. *Nat. Struct. Biol.* **2000**, *7*, 72–77.
- (14) Kay, L. E. *Nat. Struct. Biol.* **1998**, *5*, 513–517.
- (15) Fischer, M. W. F.; Majumdar, A.; Zuiderweg, E. R. P. *Prog. Nucl. Magn. Reson. Spectrosc.* **1998**, *33*, 207–272.
- (16) Korzhnev, D. M.; Billeter, M.; Arseniev, A. S.; Orekhov, V. Y. *Prog. Nucl. Magn. Reson. Spectrosc.* **2001**, *38*, 197–266.

nucleic acids, oligosaccharides, or other natural products is more difficult; therefore, heteronuclear relaxation experiments have not been used extensively for these molecules, and less is known about the internal motions of these molecules. Heteronuclear relaxation experiments probe reorientation of bond vectors of directly bound atoms; that is, they probe local motions. This means that these experiments inform only indirectly on the dynamics of nonlocal interactions, such as tertiary structure interactions in proteins, or intermolecular interactions.

NOESY or ROESY spectra yield distance restraints for structure determination by NMR. The most important cross-peaks in these spectra – long-range NOEs – are caused by nonlocal interactions. It has long been known that NOESY or ROESY cross-peak intensities are not only influenced by the (average) internuclear distance, but also by internal motions.<sup>17–21</sup> However, the influences of internuclear distance and internal motions could not be separated, with two consequences: First, the influence of internal motion on NOE intensities is not taken into account in structure determinations by solution NMR. Second, the information on internal motions that is present in NOESY and ROESY spectra is effectively discarded. To extract this information, off-resonance ROESY experiments have been proposed before.<sup>22–24</sup> However, a combined analysis is lacking of (i) what internal motions can be detected, (ii) what parameters should be measured with what precision, (iii) how this precision can be achieved, and (iv) how the data can be analyzed effectively.

Here, we present such a combined analysis of off-resonance ROESY experiments. From a realistic description of internal motions, we deduce what type of internal motions can be detected, and in molecules of what size. We describe the choice of experimental parameters for a series of off-resonance ROESY spectra, and the data analysis to detect internal motions. In the small protein BPTI, we detect internal motions of the C-terminus and of side chains that are known to be flexible. The method can detect internal motions of H,H contacts that are used in a structure calculation. Furthermore, because no isotope labeling is needed, the method works for a wide range of natural products.

## Theory

Cross-peak intensities in NOESY<sup>25</sup> or ROESY<sup>26</sup> experiments depend on NOE and ROE (cross relaxation) rates, and these rates relate to interproton distances. The NOE and ROE rates,  $\sigma_{\text{NOE}}$  and  $\sigma_{\text{ROE}}$ , can be expressed as<sup>27</sup>

$$\sigma_{\text{NOE}} = 1/20 \left( \frac{\hbar \mu_0 \gamma^2}{4\pi} \right)^2 f(r) (6J(2\omega) - J(0)) \quad (1)$$

$$\sigma_{\text{ROE}} = 1/20 \left( \frac{\hbar \mu_0 \gamma^2}{4\pi} \right)^2 f(r) (2J(0) + 3J(\omega))$$

Here,  $\hbar$  is Planck's constant,  $\gamma$  is the gyromagnetic ratio of the nuclei, and  $\mu_0$  is the vacuum permeability. The spectral density function  $J(\omega)$  describes the likelihood of spin transitions of frequency  $\omega$ . The Larmor frequency  $\omega$  is related to the static magnetic field  $B_0$  of the spectrometer by  $\omega = \gamma B_0$ . In eq 1, each cross-relaxation rate is factorized as a term  $f(r)$  and a sum of spectral density terms. The distance-dependent term  $f(r)$  depends on the average internuclear distance and on distance fluctuations (the radial component or internal motion). The spectral density terms are determined by the frequency distribution of the angular reorientation of the internuclear vector within the molecule. This frequency distribution is in turn governed by the overall tumbling of the molecule and by fluctuation of the orientation of the internuclear vector (the angular component of internal motions). The factorization of eq 1 holds if angular and radial components are not correlated.<sup>27,28</sup> It has been shown for proteins that this condition is sufficiently fulfilled for most interproton vectors.<sup>20</sup>

In the following, we discuss the influence of the angular and radial components of internal motion on NOE and ROE rates. Internal motion is commonly described by a time constant  $\tau_c$  and an order parameter  $S^2$ .<sup>29</sup> We call this order parameter  $S_\Omega^2$  to indicate that it relates to the angular component of the motion.<sup>20</sup>  $S_\Omega^2$  is a measure of the restriction of angular motion. If no angular motion is present,  $S_\Omega^2 = 1$ ; if the angular motion orients the internuclear vector randomly,  $S_\Omega^2 = 0$ . It is usually assumed that internal motions are independent of the overall tumbling of the molecule.<sup>29</sup> For spherical molecules with internal motions,  $J(\omega)$  then becomes

$$J(\omega) = 2 \left( \frac{S_\Omega^2 \tau_c}{1 + (\omega \tau_c)^2} + \frac{(1 - S_\Omega^2) \tau_c}{1 + (\omega \tau)^2} \right), \quad \frac{1}{\tau} = \frac{1}{\tau_c} + \frac{1}{\tau_e} \quad (2)$$

The rotational correlation time  $\tau_c$  describes how fast the molecule tumbles in solution. For nonspherical molecules, up to five terms of this form are needed to describe the overall tumbling of the molecule and internal motions.<sup>29,30</sup> From eqs 1 and 2 it follows how angular internal motions influence NOE and ROE rates. From the definition of  $1/\tau$  in eq 2 it follows that internal motions much slower than  $\tau_c$  do not affect  $J(\omega)$ . This reflects the physical notion that if there is an independent overall motion common to all parts of the molecule, there cannot be a component in the spectral density that decays more slowly than the overall motion.<sup>29</sup> The angular component of internal motion which is on the order of  $\tau_c$  or faster does affect  $J(\omega)$ . In the limit  $\tau_e \ll \tau_c$ , the angular component of internal motion reduces  $J(\omega)$  and, therefore, both NOE and ROE rates by  $S_\Omega^2$ . For the more general case  $\tau_e \leq \tau_c$ , the angular component of internal motions also reduces the NOE and ROE rates, but the reduction differs between NOE and ROE rates. This is the basis for the detection of internal motions described here.

(17) Davis, D. G. *J. Am. Chem. Soc.* **1987**, *109*, 3471–3472.

(18) Farmer, B. T., II; Macura, S.; Brown, L. R. *J. Magn. Reson.* **1988**, *80*, 1–22.

(19) Le Master, D. M.; Kay, L. E.; Brunger, A. T.; Prestegard, J. H. *FEBS Lett.* **1988**, *236*, 71–76.

(20) Brüschweiler, R.; Roux, B.; Blackledge, M.; Griesinger, C.; Karplus, M.; Ernst, R. R. *J. Am. Chem. Soc.* **1992**, *114*, 2289–2302.

(21) Isernia, C.; Paolillo, L.; Russo, E.; Pastore, A.; Zanutti, G.; Macura, S. *J. Biomol. NMR* **1992**, *2*, 573–582.

(22) Desvaux, H.; Berthault, P.; Birlikakis, N.; Goldman, M. *J. Magn. Reson., Ser. A* **1994**, *108*, 219–229.

(23) Kuwata, K.; Liu, H.; Schleich, T.; James, T. L. *J. Magn. Reson.* **1997**, *128*, 70–81.

(24) Malliavin, T. E.; Desvaux, H.; Aumelas, A.; Chavanieu, A.; Delsuc, M. A. *J. Magn. Reson.* **1999**, *140*, 189–199.

(25) Jeener, J.; Meier, B. H.; Bachmann, P.; Ernst, R. R. *J. Chem. Phys.* **1979**, *71*, 4546–4553.

(26) Bothner-By, A. A.; Stephens, R. L.; Lee, J.-M.; Warren, C. D.; Jeanloz, R. W. *J. Am. Chem. Soc.* **1984**, *106*, 811–813.

(27) Neuhaus, D.; Williamson, M. *The Nuclear Overhauser Effect in Structural and Conformational Analysis*; VCH Publishers: New York, 1989.

(28) Tropp, J. *J. Chem. Phys.* **1980**, *72*, 6035–6042.

(29) Lipari, G.; Szabo, A. *J. Am. Chem. Soc.* **1982**, *104*, 4546–4559.

(30) Woessner, D. E. *J. Chem. Phys.* **1962**, *37*, 647–654.

Can NOE and ROE rates reveal internal motion? Fast angular motions reduce NOE and ROE rates. Radial motions of any time scale increase NOE and ROE rates, because shorter-than-average distances have an over-proportional influence due to the high power dependence on  $r$ . Therefore, the effects of angular and radial motions on NOE and ROE rates can compensate, and molecular dynamics simulations have shown that this happens for most H,H distances.<sup>20,31</sup> Detecting internal motion from separate measurements of NOE and ROE rates is, therefore, limited to special cases.

To detect internal motion, we exploit that also the *ratio of NOE and ROE rates*,  $R = \sigma_{\text{NOE}}/\sigma_{\text{ROE}}$ , is influenced by internal motions.<sup>17,18,20,21</sup> If the angular and radial components of internal motions are not correlated, so that eq 1 holds,  $R$  becomes

$$R = \frac{\sigma_{\text{NOE}}}{\sigma_{\text{ROE}}} = \frac{6J(2\omega) - J(0)}{2J(0) + 3J(\omega)} \quad (3)$$

$R$  reports exclusively on the angular component of internal motions and is independent of the average internuclear distance and of the radial component. Therefore, no knowledge of the average internuclear distance is needed, and the problem of compensating influences of angular and radial components of internal motions is avoided. The most straightforward way to determine  $R$  is to measure NOE and ROE rates separately.<sup>17,21</sup> However, NOESY and ROESY are differently influenced by spin diffusion, and ROESY cross-peak intensities can be influenced by coherent magnetization transfer (Hartmann–Hahn transfer, TOCSY). These effects render measurements of  $R$  from separate NOESY and ROESY spectra too unreliable. These difficulties can be avoided when  $R$  is measured *directly as ratio* in off-resonance ROESY experiments.

An off-resonance ROESY experiment is characterized by a spin lock of field strength  $\gamma B_1$  and offset  $\Delta$ . In such a ROESY experiment, a spin  $i$  with chemical shift  $\Omega_i$  ( $\gamma B_1$ ,  $\Delta$ , and  $\Omega_i$  measured in Hertz relative to a common reference) will be locked at an angle (measured off the  $z$  axis)  $\theta_i$ :

$$\theta_i = \arctan(\gamma B_1 / (\Omega_i - \Delta)) \quad (4)$$

The effective cross relaxation rate  $\sigma_{\text{eff}}$  between spins  $i$  and  $j$  is a weighted average of  $\sigma_{\text{NOE}}$  and  $\sigma_{\text{ROE}}$  and depends on  $\theta_i$  and  $\theta_j$ .<sup>17,32</sup>

$$\sigma_{\text{eff}}(\theta_i, \theta_j) = \sigma_{\text{NOE}} \cos \theta_i \cos \theta_j + \sigma_{\text{ROE}} \sin \theta_i \sin \theta_j \quad (5)$$

We define the generalized spin-lock angle  $\theta$

$$\theta = \arctan \sqrt{\sin \theta_i \sin \theta_j / \cos \theta_i \cos \theta_j} \quad (6)$$

and  $c(\theta_i, \theta_j) = \sin \theta_i \sin \theta_j / \sin^2 \theta = \cos \theta_i \cos \theta_j / \cos^2 \theta$ . Equation 5 can then be rewritten as

$$\sigma_{\text{eff}}(\theta) = c(\theta_i, \theta_j)(\sigma_{\text{NOE}} \cos^2 \theta + \sigma_{\text{ROE}} \sin^2 \theta) \quad (7)$$

The scaling factor  $c(\theta_i, \theta_j) = 1$  if  $\theta_i = \theta_j$ , and is smaller than 1 for  $\theta_i \neq \theta_j$ . This reflects that cross relaxation rates are reduced for  $\theta_i \neq \theta_j$ , as compared to  $\theta_i = \theta_j$ .<sup>17,32</sup>  $\sigma_{\text{eff}}(\theta)$  describes a dispersion curve of cross-peak intensity as a function of  $\theta$ . The

extreme cases  $\theta = 0^\circ$  and  $\theta \approx 90^\circ$  correspond to unmodified NOESY and ROESY spectra. For  $0^\circ < \theta < 90^\circ$ , there is a smooth transition from NOESY to ROESY. For large ( $\omega\tau_c > \sqrt{5}/2$ ) molecules,  $\sigma_{\text{NOE}}$  and  $\sigma_{\text{ROE}}$  have opposite signs. Therefore,  $\sigma_{\text{eff}}$  becomes zero at an angle  $\theta^0$ , because NOE and ROE contributions cancel:

$$0 = \sigma_{\text{eff}}(\theta^0) = c(\theta_i, \theta_j)(\sigma_{\text{NOE}} \cos^2 \theta^0 + \sigma_{\text{ROE}} \sin^2 \theta^0) \quad (8)$$

That  $c(\theta_i, \theta_j)$  is a function of  $\theta_i$  and  $\theta_j$  does not affect  $\theta^0$ , because  $c(\theta_i, \theta_j)$  cancels out of eqs 8 and 9. At  $\theta^0$ , only the *slope*  $\partial\sigma_{\text{eff}}(\theta)/\partial\theta$  is affected by  $c(\theta_i, \theta_j)$ . It follows that  $\theta^0$  is a measure of  $R$ :

$$\frac{\sigma_{\text{NOE}}}{\sigma_{\text{ROE}}} = R = -\tan^2 \theta^0 \quad (9)$$

We conclude that  $\theta^0$  is a good quantity to measure to detect angular internal motions.

$R$  and  $\theta^0$  have been defined in terms of NOE and ROE rates, but only cross-peak intensities are experimentally accessible. Under what conditions will cross-peak intensities allow conclusions about  $R$ ? Cross-peak intensities in off-resonance ROESY spectra depend on a relaxation matrix  $R_{\text{eff}}(\Delta)$ .  $R_{\text{eff}}(\Delta)$  depends explicitly on the offset  $\Delta$ , because the  $\Delta$ -dependent angles  $\theta_i$  and  $\theta_j$  (eq 4) influence  $\sigma_{\text{eff}}(\theta_i, \theta_j)$  (eq 5). The build-up of the cross-peaks during the mixing time  $\tau_m$  is determined by the off-diagonal elements of  $R_{\text{eff}}(\Delta)$ , which are the effective cross-relaxation rates of eq 5. The diagonal elements of  $R_{\text{eff}}(\Delta)$  determine how the diagonal peaks decay during the mixing time  $\tau_m$ ; they can be described by similar equations. The intensities of an off-resonance ROESY spectrum depend on  $\Delta$  and the mixing time  $\tau_m$ :

$$I(\Delta) = I^0 \exp(-R_{\text{eff}}(\Delta)\tau_m) \quad (10)$$

A consequence of the exponential form of eq 10 is that cross-peaks due to relay transfer (spin diffusion) can be observed. If a cross-peak has a substantial spin diffusion contribution, its intensity cannot be used to reliably derive rates or conclusions about internal motions. However, spin diffusion is negligible if all off-diagonal elements of  $R_{\text{eff}}(\Delta)$  are small. Equation 10 is then well approximated by

$$I(\Delta) = I^0(1 - R_{\text{eff}}(\Delta)\tau_m) \quad (11)$$

In this linear approximation, cross-peak intensities are proportional to NOE and ROE rates. The ratio  $R$  of NOE and ROE rates can then reliably be deduced from cross-peak intensities. When does eq 11 hold? Consider the following conditions: First, internal motions are negligible (rigid molecules), so that all spin pairs have the same  $R$ . Second, the spin-lock field strength is large as compared to the spectral width ( $\gamma B_1 \gg \text{SW}$ ), so that  $\theta$  (eq 6) is constant over the spectral width. If both conditions apply, there is one offset  $\Delta$  for which all off-diagonal elements of  $R_{\text{eff}}(\Delta)$  are zero. We call this offset  $\Delta^0$ . Equation 11 holds strictly for  $\Delta^0$ , independent of the mixing time  $\tau_m$ . Thus, there is one off-resonance ROESY spectrum where all cross-peak intensities are zero. From the  $\Delta^0$  of this experiment,  $R$  can be calculated. For practical values of  $\gamma B_1$ ,  $\theta$  varies as a function of offsets within each off-resonance ROESY spectrum. As a

(31) Schneider, T. R.; Brünger, A. T.; Nilges, M. *J. Mol. Biol.* **1999**, *285*, 727–740.

(32) Griesinger, C.; Ernst, R. R. *J. Magn. Reson.* **1987**, *75*, 261–271.

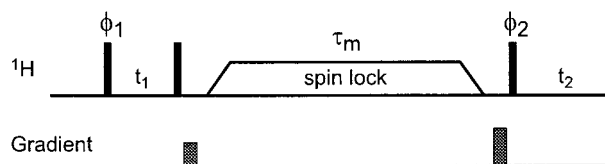


**Figure 1.** Pulse sequence for off-resonance ROESY experiments. The ROESY spin lock is implemented as adiabatic pulse which rotates magnetization from the  $z$  axis to the spin-lock axis.<sup>30,31</sup> Pulse phases are  $x$ , except  $\phi_1 = x, -x$ ;  $\phi_2 = x, x, y, y, -x, -x, -y, -y$ ; receiver =  $x, -x, y, -y, -x, x, -y, y$ .

consequence, not all off-diagonal elements are zero for  $\Delta^0$ , but they are scaled down near  $\Delta^0$ , and eq 11 can remain a good approximation. Internal motion has a similar effect, that not all cross-peaks are zero for  $\Delta^0$ , but again the off-diagonal elements are scaled down near  $\Delta^0$ . In the next section, we describe experimental parameter settings needed to make eq 11 a good enough approximation, so that  $\theta^0$  can be derived from cross-peak intensities and internal motions can be detected.

### General Experimental Procedure

To detect internal motions, we record a series of off-resonance ROESY spectra that differ in  $\Delta$ . For each cross-peak, these spectra yield a series of intensities as a function of  $\theta$  (defined in eq 6), from which  $\theta^0$  is derived. Parameters for these spectra must be chosen so that cross-peak intensities around  $\theta^0$  are systematically sampled. In particular, the zero crossing must be observed for all cross-peaks, irrespective of the offsets of the interacting spins. The parameters are chosen so that the precision of the  $\theta^0$  measurements is maximized, because differences in  $\theta^0$  are related to internal motion (see Results).

To record off-resonance ROESY spectra, the  $z$ -filtered ROESY pulse sequence shown in Figure 1 is used. The ROESY spin lock during the mixing time is implemented as a shaped pulse. The shape consists of a middle section of constant amplitude, and begins and ends with “adiabatic ramps” of 2 ms duration and shaped as  $\sin^2(x)$  ( $0 < x < \pi/2$ ). These ramps prevent magnetization losses at the beginning and end of the spin lock.<sup>33,34</sup> Two gradient pulses of unequal strength are added before and after the spin lock to ensure that purely absorptive spectra are obtained. A mixing time toward the end of the linear NOE build-up can be chosen. The starting value of  $t_1$  is set so that the zero- and first-order phase corrections in the incremented dimension are  $90^\circ$  and  $-180^\circ$ , respectively.<sup>35</sup> Presaturation can be used to suppress the solvent signal. The variation of  $\theta$  is achieved by varying the offset  $\Delta$  of the spin lock between the experiments, while the spin-lock field strength  $\gamma B_1$  is kept constant. This maximizes the precision of  $\theta^0$  measurements, because  $\Delta$  can be set more precisely than  $\gamma B_1$ , and constant  $\gamma B_1$  ensures equal sample heating in all experiments, making them more comparable. The spin-lock field strength must be chosen so that eq 11 becomes a good approximation. As high a field strength as is compatible with good instrument stability can be used. A field strength (in Hz) 50–100% larger than the chemical shift range (in Hz) is sufficient. For example, the chemical shift range of BPTI in our experiments was about 5000 Hz, and we used  $\gamma B_1$  of 7180 or 10 970 Hz (see below).  $\gamma B_1$  is measured simply by calibration of a low-power  $180^\circ$  pulse, because accurate knowledge of  $\gamma B_1$  is not needed. Note that these field strengths will induce some sample heating, especially for samples with high ionic strength. The field strength that can be used might also be limited by the radio frequency power that the probe can tolerate. These points did not present problems on our system, equipped with a regular probe.

We define the spin-lock angle in the middle of the spectrum as  $\theta_{\text{exp}}$ , as a way to refer to off-resonance ROESY experiments. To determine which range of  $\theta_{\text{exp}}$  must be sampled to measure  $\theta^0$ , two test spectra with  $\theta_{\text{exp}} = 10^\circ$  and  $40^\circ$  are acquired. Cross-peaks close to the center of these spectra must have opposite signs. This will generally be fulfilled for molecules of at least 2 kDa molecular mass. For smaller molecules, the temperature can be lowered, or a viscous cosolvent can be added to increase the correlation time. An estimate of  $\theta^0$  is then interpolated from the ratio of the intensities of a number of cross-peaks in the center of the test spectra. This estimate of  $\theta^0$  becomes the center of a  $20^\circ$  range of  $\theta_{\text{exp}}$  values that are sampled. For example, if the estimated  $\theta^0$  is  $32^\circ$ , spectra with  $\theta_{\text{exp}} = 23, 26, 29, 32, 35, 38, 41^\circ$  might be recorded. The offsets  $\Delta$  needed for these  $\theta_{\text{exp}}$  are calculated using eq 4 ( $\Omega =$  center of the spectrum) and the measured  $\gamma B_1$ . The offset  $\Delta$  for each experiment is realized by switching the  $^1\text{H}$  carrier from the center of the spectrum to frequency  $\Delta$  during the spin lock. All spectra of a series are processed in the same way. After baseline correction in both dimensions, signal intensities are obtained by integration of cross-peak volumes. For each cross-peak in each spectrum,  $\theta$  is calculated using eqs 4 and 6. The series of experiments yields for each cross-peak a series of integrals as a function of angle  $\theta$ . The zero crossing of the series of intensities defines  $\theta^0$  (eq 8).  $\theta^0$  is found by fitting a second-order polynomial to the series of intensities as a function of  $\theta$ . A script for the Matlab program package for these calculations is available as Supporting Information S5.

Cross-relaxation cross-peaks between scalar coupled spins have a contribution due to transfer of zero quanta during the mixing time. This leads to antiphase contributions to the cross-peaks which are dispersive in both dimensions (COSY-type cross-peaks<sup>36</sup>). Because these contributions have zero integrated intensity, they do not hamper the interpretation of off-resonance ROESY spectra if peak integrals, rather than intensities, are analyzed. A method to eliminate antiphase contributions has been proposed.<sup>37</sup>

Two independent series of off-resonance ROESY spectra were recorded at  $45^\circ\text{C}$  on a Bruker AMXII 500 NMR spectrometer, equipped with a  $^1\text{H}$ ,  $^{13}\text{C}$ ,  $^{15}\text{N}$  probe with a shielded  $z$ -gradient, on a 10 mM sample of BPTI in  $\text{H}_2\text{O}/\text{D}_2\text{O}$  90:10. The relaxation delay (with presaturation of the water resonance) was 2.9 s (two longitudinal relaxation times of the slowest-relaxing nuclei). The mixing time was 130 ms. For each experiment, 200 complex  $t_1$  data points of 48 scans each were collected; the total experiment time for each series of experiments was about 2.5 days. The first series of seven spectra was recorded with  $\theta_{\text{exp}}$  spaced equally between  $25^\circ$  and  $49^\circ$  and a  $\gamma B_1$  of 7180 Hz. In the second series of eight experiments,  $\theta_{\text{exp}}$  was spaced equally between  $26^\circ$  and  $47^\circ$ , and  $\gamma B_1$  was 10 970 Hz. The spectra were processed using the XWINNMR program package. The raw data were extended by 50% by linear prediction in  $t_1$ , apodized with shifted squared sine bells in both dimensions, and Fourier transformed after zero-filling in both dimensions. Baseline correction and integration of the cross-peaks were also done with XWINNMR. In addition, a series of eight off-resonance ROESY spectra was recorded at  $29^\circ\text{C}$  on the same spectrometer on a 3 mM sample of a DNA three-way junction (3WJ1)<sup>38</sup> in  $\text{D}_2\text{O}$  at pH 6.9 (total experiment time: 4 days).

### Results

In the Theory section, we described how the angular and radial components of internal motion influence NOE and ROE rates. In principle, internal motions could be detected as deviations of experimental NOE or ROE rates from rates expected for a rigid molecule. However, this would require unrealistically precise knowledge of the average internuclear

(33) Dezheng, Z.; Fujiwara, T.; Nagayama, K. *J. Magn. Reson.* **1989**, *81*, 628–630.

(34) Desvaux, H.; Berthault, P.; Birlirakis, N.; Goldman, M.; Piotto, M. *J. Magn. Reson., Ser. A* **1995**, *113*, 47–52.

(35) Bax, A.; Ikura, M.; Kay, L. E.; Zhu, G. *J. Magn. Reson.* **1991**, *91*, 174–178.

(36) Bax, A.; Davis, D. G. *J. Magn. Reson.* **1985**, *63*, 207–213.

(37) Davis, A. L.; Estcourt, G.; Keeler, J.; Laue, E. D.; Titman, J. J. *J. Magn. Reson., Ser. A* **1993**, *105*, 167–183.

(38) Van Buuren, B. N. M.; Overmars, F. J. J.; Ippel, J. H.; Altona, C.; Wijmenga, S. S. *J. Mol. Biol.* **2000**, *304*, 371–383.

distance and of  $\tau_c$ . Furthermore, even if the distance and  $\tau_c$  are known, NOE or ROE rates may not reveal internal motion, because radial and angular components can have compensating influences on the rates. Molecular dynamics simulations have shown that this compensation occurs for most H,H distances.<sup>20,31</sup> In contrast, the *ratio*  $R$  of NOE and ROE rates is not affected by this compensation, because it is only affected by the angular component (eqs 1, 3). We concluded in the Theory section that to achieve sufficient precision,  $R$  must be measured in an experiment that is directly sensitive to  $R$ , such as off-resonance ROESY experiments.

Off-resonance ROESY experiments, which measure a weighted average of NOE and ROE rates, have previously been proposed to detect internal motion.<sup>22–24</sup> In these experiments, the weight of NOE and ROE can be described and experimentally set by an angle  $\theta$  (eq 6). As a function of  $\theta$ , the cross-peak intensities in these experiments have a zero crossing at an angle  $\theta^0$ , which is related to the ratio  $R$  of NOE and ROE rates (eqs 8, 9). In the General Experimental Procedure section, we described the choice of parameters for a series of off-resonance ROESY experiments to measure  $\theta^0$ . These parameters are chosen so that the initial rate approximation (eq 11) holds. We noted that  $\theta^0$  is sensitive to the angular component of internal motion, but insensitive to the radial component. We describe the angular component by a correlation time  $\tau_e$  and an angular order parameter  $S_{\Omega}^2$ .<sup>29</sup> It follows from eqs 2 and 3 that  $\theta^0$  depends on  $\tau_e$ ,  $S_{\Omega}^2$ , the rotational correlation time  $\tau_c$ , and the spectrometer frequency  $\omega$ . In Figure 2, we display for spectrometer frequencies of 500 MHz (Figure 2A) and 800 MHz (Figure 2B) how  $\theta^0$  depends on  $\tau_e$  and  $S_{\Omega}^2$ . At the top of each panel, the  $\theta^0$  predicted for a rigid molecule with  $\tau_c = 2$  ns is indicated. The iso-lines of  $\theta^0$  show which combinations of  $\tau_e$  and  $S_{\Omega}^2$  produce the same  $\theta^0$ . Increasing internal motion, expressed as decreasing  $S_{\Omega}^2$ , causes decreasing  $\theta^0$ . It becomes clear that *differences* in  $\theta^0$  relate to internal motion, from which follows that *only differences* in  $\theta^0$  have to be measured accurately. Brüschweiler et al. showed that two criteria determine the sensitivity of the ratio  $R$  to internal motions.<sup>20</sup> Analogous conditions hold for  $\theta^0$ , which are visible in Figure 2. First, for any order parameter  $S_{\Omega}^2$ , internal motion affects  $\theta^0$  strongest if  $\omega\tau_e \approx 1$  ( $\tau_e$  approximately 150 ps for 500 MHz proton resonance frequency). For smaller and larger  $\tau_e$ ,  $\theta^0$  becomes less sensitive to internal motion. This holds independent of  $\omega\tau_c$ . Second, the overall sensitivity of  $\theta^0$  to internal motions decreases when  $\omega\tau_c$  increases.  $\theta^0$  is most sensitive to internal motion when  $\omega\tau_c$  is slightly above 1. For example, for  $\tau_c = 2$  ns, an internal motion with  $S_{\Omega}^2 = 0.5$  reduces  $\theta^0$  at most by 4.3° for  $\omega/2\pi = 500$  MHz ( $\omega\tau_c = 6.3$ ), but only by 2.7° for 800 MHz ( $\omega\tau_c = 10$ ). The decrease of the sensitivity of  $\theta^0$  to internal motion with increasing  $\omega\tau_c$  implies that there is an upper limit  $\omega\tau_c \approx 40$  for the effective detection of internal motion by off-resonance ROESY. For usual spectrometer frequencies, this corresponds to a maximum correlation time  $\tau_c$  of about 10 ns, or a maximum molecular weight of about 15 kDa. For large molecules, the detection of internal motion will be more sensitive at lower spectrometer frequencies.

A measurement of  $\theta^0$  at one spectrometer frequency defines a contour in a  $S_{\Omega}^2$ ,  $\tau_e$  plane such as Figure 2A.  $\tau_e$  and  $S_{\Omega}^2$  cannot be separated from a measurement of  $\theta^0$  at a single field strength, but an upper limit of  $S_{\Omega}^2$  can be derived. Measurements of  $\theta^0$  at

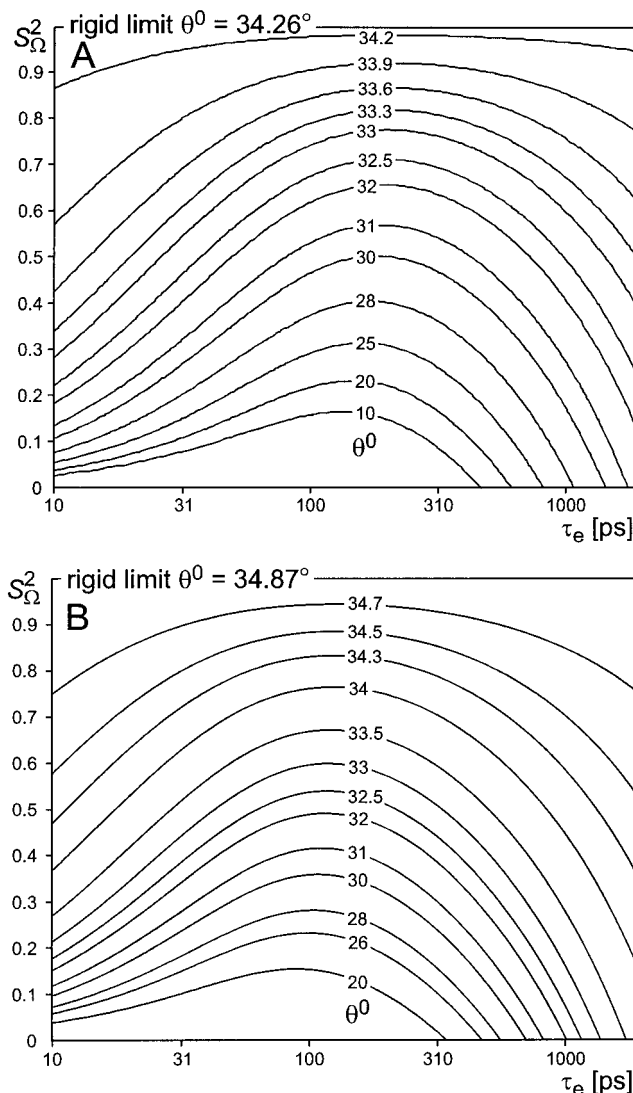


**Figure 2.** Iso-lines of  $\theta^0$  as function of  $\tau_e$  and  $S_{\Omega}^2$ . Simulations used eqs 1, 2, 9 and assumed a correlation time  $\tau_c = 2$  ns and spectrometer frequencies of (A) 500 MHz and (B) 800 MHz. Reduced  $\theta^0$  indicates angular internal motion, but  $\tau_e$  and  $S_{\Omega}^2$  cannot be separated by measurements of  $\theta^0$  at one spectrometer frequency.

two spectrometer frequencies will yield differing  $\theta^0$  values, which each define a contour of possible  $S_{\Omega}^2$  and  $\tau_e$ . These contours intersect in one point, and this intersection allows one to estimate  $S_{\Omega}^2$  and  $\tau_e$ . For example, a  $\theta^0$  of 32.5° at 500 MHz is compatible with the  $S_{\Omega}^2/\tau_e$  combinations 0.72/200 ps or 0.45/31 ps (Figure 2A). These  $S_{\Omega}^2/\tau_e$  combinations lie on the 33.7° and 33.0° contours at 800 MHz (Figure 2B), which allows one to distinguish the  $S_{\Omega}^2/\tau_e$  combinations.

We recorded two series of off-resonance ROESY spectra on the small protein BPTI. The parameters of the spectra are given in the General Experimental Procedure section. Figure 3 displays the integrals of the cross-peaks F22H<sup>N</sup>,Y21H<sup>α</sup> (rigid  $\beta$ -sheet of BPTI) and A58H<sup>N</sup>,G57H<sup>α</sup> (mobile C-terminus), as a function of the angle  $\theta$  of the individual cross-peaks. Figure 3 also displays the second-order polynomials that were fit to each series of data. The zero crossings of the polynomials for the F22H<sup>N</sup>,Y21H<sup>α</sup> and A58H<sup>N</sup>,G57H<sup>α</sup> cross-peaks are  $\theta^0 = 37.3^\circ$  and  $33.4^\circ$ , respectively.

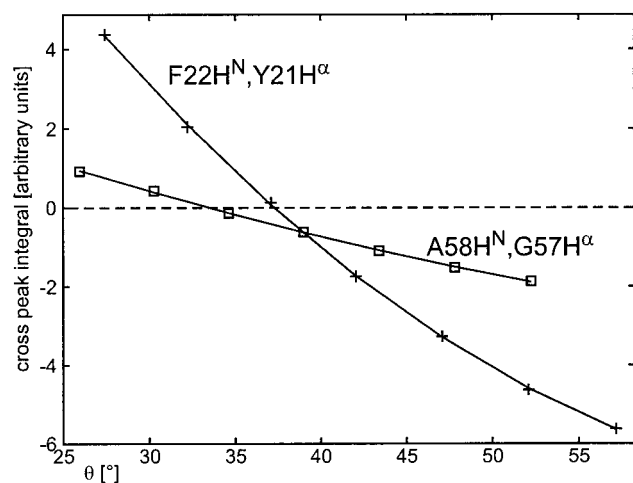


**Figure 3.** Experimental cross-peak integrals and second-order polynomial fit of the integrals as a function of  $\theta$ . Crosses: Sequential F22H<sup>N</sup>,Y21H<sup>α</sup> cross-peak in the rigid  $\beta$ -sheet of BPTI. Squares: Sequential C-terminal A58H<sup>N</sup>,G57H<sup>α</sup> cross-peak, which shows a lower zero-crossing angle  $\theta^0$ , due to the flexibility of the C-terminus. Positive intensities indicate NOESY behavior; negative intensities indicate ROESY behavior. The  $x$  axis values of the experimental points differ between the cross-peaks, because the chemical shifts of the two interacting spins enter the calculation of  $\theta$  (eq 6).

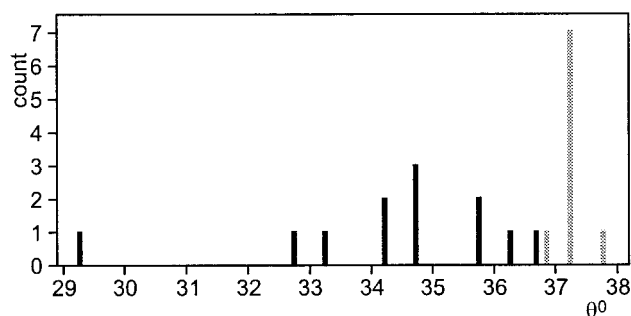


**Figure 4.** Histogram of zero-crossing angles  $\theta^0$  of H<sup>α</sup>,H<sup>β</sup> cross-peaks of well-defined (shaded bars) and flexible (solid bars) side chains.  $\theta^0$  values were grouped in intervals of 0.5°. Cross-peaks in well-defined side chains have high  $\theta^0$  values in a narrow range, while flexible side chains have lower and more variable  $\theta^0$  values.

Using the first series of seven spectra, we analyzed the zero-crossing angles  $\theta^0$  of all resolved H<sup>N</sup>,H<sup>α</sup> cross-peaks in the main secondary structural elements of BPTI. For the antiparallel  $\beta$ -sheet, the  $\theta^0$  values were  $(37.6 \pm 0.3)^\circ$  ( $37.3$ – $38.2^\circ$ ,  $n = 21$ ). The  $\theta^0$  values found for cross-peaks above and below the diagonal agreed to  $\pm 0.25^\circ$ , and there was no significant difference in  $\theta^0$  between intra- and interresidue cross-peaks. H<sup>N</sup>,H<sup>α</sup> cross-peaks in the  $\alpha$ -helix showed the same average  $\theta^0$  ( $37.5 \pm 0.5)^\circ$  ( $36.7$ – $38.7^\circ$ ,  $n = 13$ ). Thus, the  $\theta^0$  values of H<sup>N</sup>,H<sup>α</sup> cross-peaks in regular secondary structures fall into a narrow range. They are also the highest observed  $\theta^0$  values. To test the applicability of the method to side-chain hydrogen pairs, we analyzed intraresidue H<sup>α</sup>,H<sup>β</sup> cross-peaks and long-range NOEs. As shown in Figure 4, H<sup>α</sup>,H<sup>β</sup> cross-peaks of side chains with a well-defined conformation in the NMR structure of BPTI<sup>39</sup> showed  $\theta^0 = (37.3 \pm 0.3)^\circ$  ( $36.7$ – $37.8^\circ$ ,  $n = 9$ ; Supporting Information Table S1). We defined side chains as flexible if they showed averaged H<sup>α</sup>,H<sup>β</sup> coupling constants,<sup>39</sup> or were solvent-exposed, as judged from the X-ray structure.<sup>40</sup> H<sup>α</sup>,H<sup>β</sup>

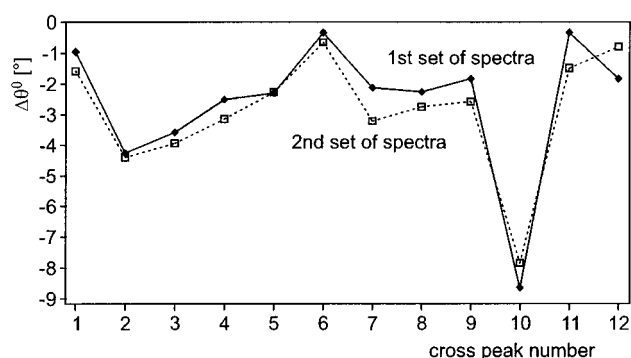


**Figure 5.** Reproducibility of reductions of  $\theta^0$  due to internal motions. For H<sup>α</sup>,H<sup>β</sup> cross-peaks, the plot shows differences between  $\theta^0$  of individual flexible side chains, and the average  $\theta^0$  of well-defined side chains. Diamonds and filled line: First series of off-resonance ROESY spectra. Open squares and broken line: Second series of off-resonance ROESY spectra. Differences in  $\theta^0$  between cross-peaks are well reproduced.

cross-peaks of these flexible side chains showed smaller  $\theta^0$  values and a larger spread in  $\theta^0$  ( $34.3 \pm 1.9)^\circ$  ( $29.4$ – $36.6^\circ$ ,  $n = 12$ ; Supporting Information Table S2). The C-terminal residues G57 and A58 showed  $\theta^0$  of  $33.4^\circ$  (interresidue A58H<sup>N</sup>,G57H<sup>α</sup> cross-peak, Figure 3) and  $29.4^\circ$  (intraresidue A58H<sup>α</sup>,A58H<sup>β</sup> cross-peak). We analyzed 29 easily identifiable and well-resolved long-range NOEs. Of these, the NOEs not involving methyl groups showed  $\theta^0 = (37.2 \pm 0.55)^\circ$  ( $35.6$ – $38.0^\circ$ ,  $n = 19$ ; Supporting Information Table S3). NOEs involving methyl groups showed  $\theta^0 = (36.4 \pm 0.3)^\circ$  ( $35.9$ – $37.2^\circ$ ,  $n = 10$ ; Supporting Information Table S4).

We used the second independent series of spectra to test the reproducibility of  $\theta^0$  measurements. We compared  $\theta^0$  values of H<sup>α</sup>,H<sup>β</sup> cross-peaks of rigid and flexible side chains. The  $\theta^0$  values of H<sup>α</sup>,H<sup>β</sup> cross-peaks in rigid and flexible side chains differed significantly between the first and second series of spectra. For the rigid side chains, the average  $\theta^0$  values were  $37.3^\circ$  (first series) and  $36.5^\circ$  (second series). However, only differences in  $\theta^0$  are important for the detection of internal motion. As shown in Figure 5, differences between the average  $\theta^0$  of rigid side chains and the  $\theta^0$  values of individual flexible side chains are well reproduced. We also recorded a series of off-resonance ROESY spectra on a 3 mM sample of a DNA three-way junction (3WJ1, 36 nucleotides, molecular weight 11 kDa).<sup>38</sup> These spectra showed variation in  $\theta^0$  of approximately  $4^\circ$ , and the precision was  $0.25^\circ$ .

## Discussion

It has long been known that the ratio of NOE and ROE rates,  $R$ , can report on internal motions.<sup>17,18,20,21</sup> Davis<sup>17</sup> measured NOE and ROE rates separately from NOE and ROE build-up curves and estimated  $\tau_c$  and  $r$ . Isernia et al.<sup>21</sup> averaged NOE and ROE rates of several cross-peaks to determine an average  $\tau_c$ . This estimate of  $\tau_c$  was used to calculate internuclear distances. Isernia et al. did not attempt to extract information on motions of individual H,H contacts.

Two approaches have been described to derive internal motion from off-resonance ROESY spectra. In the first approach, Kuwata et al.<sup>23</sup> fitted the dispersion curve  $\sigma_{\text{eff}}(\theta_r, \theta_j)$  to models containing  $r$ ,  $S^2$ ,  $\tau_c$ , or an effective correlation time  $\tau_{\text{eff}}$  as variables. The whole dispersion curve  $\sigma_{\text{eff}}(\theta)$  for  $0^\circ \leq \theta \leq 90^\circ$

(39) Berndt, K. D.; Güntert, P.; Orbons, L. P. M.; Wüthrich, K. *J. Mol. Biol.* **1992**, *227*, 757–775.

(40) Deisenhofer, J.; Steigemann, W. *Acta Crystallogr., Sect. B* **1975**, *31*, 238–250.

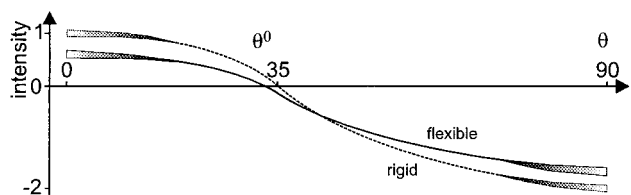


**Figure 6.** Schematic display of cross-peak intensities in NOESY ( $\theta = 0^\circ$ ), off-resonance ROESY ( $\theta \approx 35^\circ$ ), and ROESY ( $\theta \approx 90^\circ$ ) experiments. As compared to a rigid molecule (broken line), NOESY and ROESY cross-peak intensities are reduced in the presence of angular internal motion (solid line), and  $\theta^0$  is reduced. The ratio of NOESY and ROESY intensities is hard to measure, because these intensities are influenced by spin diffusion and TOCSY (indicated by shading). In contrast,  $\theta^0$  can be determined with good precision, because spin diffusion is negligible in the vicinity of  $\theta^0$ .

depends on the average distance, on  $\tau_c$ , and on the radial and angular components of internal motions. These parameters, and in particular radial motions and the average distance, cannot all be separated. In contrast, variation of  $\theta^0$  is caused exclusively by the angular component of internal motions. Therefore, we do not attempt to derive  $r$ , but concentrate on the detection of the angular component of internal motion from precise measurements of  $\theta^0$ . To measure  $\theta^0$ , we record a series of off-resonance ROESY experiments over a small range of  $\theta_{\text{exp}}$  around the expected  $\theta^0$ . This has two advantages (Figure 6): First, TOCSY transfer can be neglected (unless spins are strongly coupled even without spin lock), because the  $z$  component of the spin-locked magnetization is large.<sup>41</sup> If a pair of strongly coupled spins has cross-peaks to a third spin, TOCSY transfer can average the  $\theta^0$  values of these cross-peaks, but the averaged  $\theta^0$  values remain meaningful. Second, the effective cross relaxation rates (eq 7) are small for  $\theta_{\text{exp}} \approx \theta^0$ , so that cross-peak intensities are only little influenced by spin diffusion.

In the second approach to derive internal motion from off-resonance ROESY spectra, Malliavin et al.<sup>24</sup> described a method to analyze off-resonance ROESY spectra acquired with several  $\theta_{\text{exp}}$  and one or two mixing times. Their analysis yields NOE and ROE rates, the ratio of which was visualized as zero-crossing angles. Malliavin et al. used a JS-ROESY pulse sequence.<sup>42,43</sup> These pulse sequences effectively average two spectra, so that the dependence of  $\sigma_{\text{eff}}$  on the chemical shifts of the two interacting spins (eq 5) appears reduced. However, the chemical shift dependence cannot be eliminated, and its size varies with  $\theta_{\text{exp}}$ . This means that  $\theta$  is not known with sufficient precision to determine  $\theta^0$  with a precision of a fraction of  $1^\circ$ . Therefore, the chemical shift dependence cannot be ignored. We, therefore, use the pulse sequence of Figure 1, which does not reduce the chemical shift dependence, but allows us to treat it explicitly. This we achieve through the definition of  $\theta$  (eq 6), which allows the cross-peak intensities to be analyzed as a function of *one* variable, although  $\sigma_{\text{eff}}$  depends on *two* chemical shifts.

**Effect of Spin Diffusion.** Spin diffusion can degrade the accuracy of  $\theta^0$  measurements. In spin diffusion, cross-peak intensity is transferred from spin A, via spin B, to spin C. An A,C cross-peak is observed, although the A,C distance is long. Such spin-diffusion-mediated cross-peaks cannot be analyzed

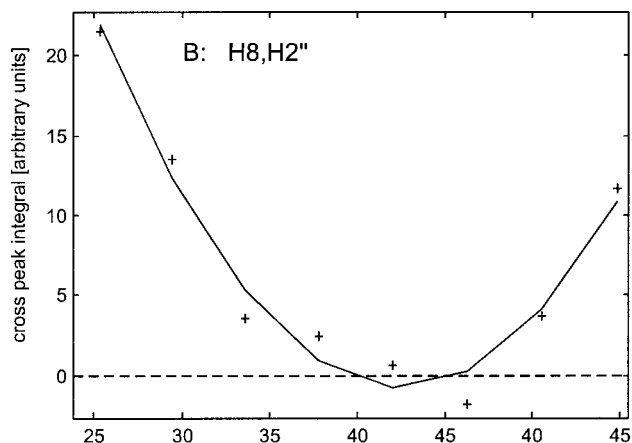
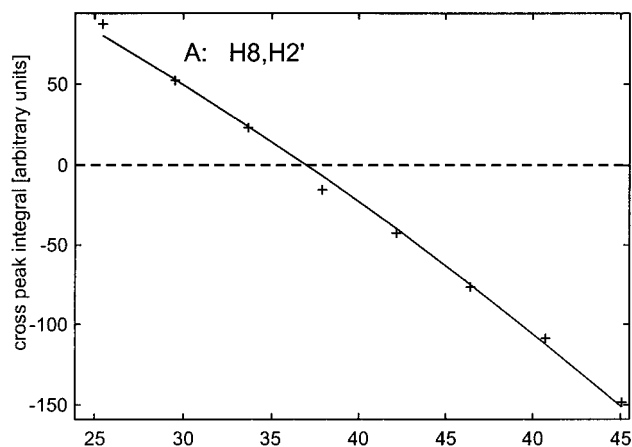


**Figure 7.** Experimental cross-peak integrals in a DNA three-way junction as a function of  $\theta$ . (A) The H8,H2' cross-peak is a direct NOE, shows a zero crossing, and the integrals are fit well by a second-order polynomial. (B) The H8,H2'' cross-peak does not show a well-defined zero crossing, and the integrals are poorly fit by a second-order polynomial, revealing that this cross-peak is mainly mediated by spin diffusion via H2'. Note the different scaling of the cross-peak integrals.

using the initial rate approximation (eq 11). The strong NOE between methylene protons is the most serious cause of spin diffusion. To estimate the influence of spin diffusion on  $\theta^0$ , we carried out simulations for an amino acid  $H^\alpha, H^\beta, H^\beta'$  spin system and for a nucleotide H8,H2',H2'' spin system. We assumed that the  $H^\alpha, H^\beta$  or H8,H2' distance is short and the  $H^\alpha, H^\beta'$  or H8,-H2'' distance is long. The former cross-peaks are direct, the latter mainly spin-diffusion mediated. The simulations (for a mixing time of 100 ms and  $\tau_c = 7$  ns) showed that for the direct cross-peaks, spin diffusion within the respective methylene group leads to deviations of  $\theta^0$  of less than  $0.1^\circ$ . Larger errors in  $\theta^0$  occur for the H8,H2'' cross-peak. In practice, cross-peaks that are mostly mediated by spin diffusion can easily be recognized by a characteristic dependence of the cross-peak intensity on  $\theta$ . Instead of the normal NOE–ROE cross over (Figure 7A), the intensities level off for higher values of  $\theta$ , or become positive again, as displayed in Figure 7B for a H8,H2'' cross-peak in the DNA three-way junction 3WJ1. The intensities of the spin-diffusion mediated H8,H2'' cross-peaks could not be properly fitted by a second-order polynomial (Figure 7B). Internal motions between spins that have a mainly spin-diffusion mediated interaction are difficult to interpret if all involved atoms are freely mobile, because the relative motion of three

(41) Schleucher, J.; Quant, J.; Glaser, S. J.; Griesinger, C. In *Encyclopedia of NMR*; Grant, D. M., Harris, R. K., Eds.; Wiley: New York, 1996; Vol. 8, pp 4789–4804.

(42) Schleucher, J.; Quant, J.; Glaser, S. J.; Griesinger, C. *J. Magn. Reson., Ser. A* **1995**, *112*, 144–151.

(43) Desvaux, H.; Goldman, M. *J. Magn. Reson., Ser. B* **1996**, *110*, 198–201.

atoms must be considered. On the other hand, in cases such as  $H^\alpha, H^\beta, H^\gamma$ , it is likely that the  $\theta^0$  of the direct  $H^\alpha, H^\beta$  cross-peak reveals most internal motion, simply because the  $C^\beta H_2$  group is a rigid system. We propose to restrict the analysis to direct cross-peaks, such as the stronger cross-peak of a methylene group. Spin-diffusion-mediated cross-peaks can be identified from a structure of the investigated molecule, which typically will be known when internal motions are analyzed.

**Precision and Accuracy of  $\theta^0$  Measurements.** To vary the spin-lock angles between experiments, we chose to vary  $\Delta$  at constant  $\gamma B_1$ . This amounts to maximizing the precision of  $\theta^0$  (see General Experimental Procedure). To estimate the precision, we compared  $\theta^0$  values of symmetry-related  $H^N, H^\alpha$  cross-peaks of the  $\beta$ -sheet of BPTI. The agreement of  $0.25^\circ$  between these  $\theta^0$  values showed that  $\theta^0$  can be measured with a precision of  $0.25^\circ$ , which is sufficient to detect changes in  $\theta^0$  of the expected magnitude (Figure 2).

To estimate what signal-to-noise ratio is needed to measure  $\theta^0$ , we added noise to a series of cross-peak intensities and determined  $\theta^0$ . The standard deviation of the resulting  $\theta^0$  values indicated that  $\theta^0$  can be measured with  $0.25^\circ$  precision if the largest intensity of a series has a signal-to-noise ratio of at least 30:1. From eq 5 we estimate that cross-peaks in the most intense off-resonance ROESY spectra (with the extreme values  $\theta_{\text{exp}} \approx \theta^0 \pm 10^\circ$ ) have about one-half the intensity of a NOESY spectrum ( $\theta_{\text{exp}} = 0^\circ$ ). Therefore, cross-peaks can be analyzed with off-resonance ROESY if they have a signal-to-noise ratio of 30:1 in a NOESY with one-half as long of a mixing time.

We used the two independent series of off-resonance ROESY spectra to test the accuracy of measurements of  $\theta^0$ . In the two series of spectra, rigid  $H^\alpha, H^\beta$  cross-peaks showed average  $\theta^0$  values of  $37.2$  and  $36.5^\circ$ . Under the conditions of our experiments, BPTI has a correlation time of  $\tau_c \approx 2$  ns,<sup>44</sup> corresponding to a maximum rigid-molecule  $\theta^0$  of  $34.26^\circ$  (Figure 2A). Furthermore, the theoretical maximum  $\theta^0$  is  $35.26^\circ$  (for  $\omega\tau_c \gg 1$ ). Therefore, the high  $\theta^0$  values of  $37.3^\circ$  and  $36.5^\circ$  must be explained. First, a deviation of the measured  $\theta^0$  from the true value is caused by the duration of the gradients and adiabatic ramps during the mixing time. These durations act as NOESY mixing times, which lead to a systematic overestimation of  $\theta^0$  by about  $0.7^\circ$ . Furthermore,  $\gamma B_1$  is not constant over the sample volume ("B<sub>1</sub> inhomogeneity"), which also leads to an overestimation of  $\theta^0$  by more than  $1^\circ$  (not shown). Both effects together explain the overestimation of  $\theta^0$ . The average  $\theta^0$  values of rigid side chains differed systematically by  $0.8^\circ$  ( $37.3$  and  $36.5^\circ$ ) between the two series of spectra. This difference can be explained by a realistic 3% uncertainty in the measurement of  $\gamma B_1$ . The difference is of no consequence, because we want to precisely measure *differences* of  $\theta^0$  between rigid and flexible groups. For both series of spectra, Figure 5 shows the reduction of  $\theta^0$  for flexible side chains, as compared to rigid side chains. These differences are well reproducible. In summary, the accuracy of  $\theta^0$  is lower than the precision, but the precision is sufficient to detect *differences* in  $\theta^0$  caused by internal motions.

**Results for BPTI.** In the first series of spectra, we analyzed inter- and intraresidue  $H^N, H^\alpha$  cross-peaks in the  $\beta$ -sheet and the  $\alpha$ -helix, and  $H^\alpha, H^\beta$  cross-peaks of structurally well-defined side chains. These groups of cross-peaks showed very similar

average  $\theta^0$  values of  $37.6^\circ$ ,  $37.5^\circ$ , and  $37.3^\circ$ . This indicates that there is a well-defined maximal  $\theta^0$ , which represents the overall tumbling of the molecule. Long-range NOEs not involving methyl groups showed an average  $\theta^0$  value of  $37.2^\circ$  (Supporting Information Table S3). This implies that in BPTI, long-range NOEs do not have more angular motions than do backbone NOEs. Significantly reduced  $\theta^0$  values were observed for the C-terminus and flexible side chains (Figure 4), indicating internal motions. The  $\theta^0$  values of  $H^\alpha, H^\beta$  NOEs of flexible side chains are reduced by approximately  $2^\circ$ , showing that side-chain rotations reduce the order parameters of these  $H^\alpha, H^\beta$  vectors to  $S_\Omega^2 \leq 0.6$ . Long-range NOEs involving methyl groups showed an average  $\theta^0$  value of  $36.4^\circ$ , only about  $1^\circ$  lower than rigid NOEs. That methyl rotation causes only a small reduction of  $\theta^0$  is expected, because it is faster (25 ps)<sup>45</sup> than the most  $\theta^0$ -sensitive time scale (150 ps).

Heteronuclear relaxation studies and off-resonance ROESY detect different components of internal motion. First, heteronuclear relaxation is sensitive to motions from picoseconds to milliseconds, while  $\theta^0$  probes motions on the 100 ps time scale. Second, motions of different vectors are probed, X,H bond vectors by heteronuclear relaxation and H,H vectors by off-resonance ROESY. Therefore, X,H order parameters are not directly comparable to order parameters derived from  $\theta^0$ . <sup>15</sup>N relaxation studies indicate little fast backbone motion in BPTI, except for the C-terminal residues G57 and A58.<sup>44,46</sup> Nirmala and Wagner observed larger  $T_1$  values of  $C^\alpha$  atoms of amino acids 15, 24–26, 58, which agreed with expected higher flexibility of these amino acids, but no order parameters were given.<sup>47</sup> We observed reduced  $\theta^0$  values for cross-peaks involving amino acids 26, 57, 58. Furthermore, the reduction of  $\theta^0$  values of side chains agrees with known side-chain flexibility (Figure 4). Our results, therefore, agree with previous results as far as a comparison is possible.

**Scope and Limitations.** The sensitivity of  $\theta^0$  for internal motions declines with increasing  $\omega\tau_c$  (Figure 2), so it becomes more difficult to detect internal motions for larger molecules. We observed reductions of  $\theta^0$  of more than  $4^\circ$  in BPTI, and up to  $4^\circ$  in the DNA three-way-junction 3WJ1<sup>38</sup> of 11 kDa molecular weight ( $\omega\tau_c \approx 20$ ). The sample of 3WJ1 was 3 mM, the experiment time was 4 days, and the precision of  $\theta^0$  was  $0.25^\circ$ . This suggests that molecules up to at least 15 kDa can be studied with H,H off-resonance ROESY to detect internal motions. This molecular weight limit might be extended severalfold using <sup>13</sup>C,<sup>13</sup>C cross relaxation.

Can off-resonance ROESY be used to correct estimates of internuclear distances for internal motion? From  $\theta^0$  an upper limit of  $S_\Omega^2$  can be estimated, which tells for each H,H contact how much the NOE and ROE rates are reduced by angular motion. From  $S_\Omega^2$  and measured NOE rates the value of  $f(r)$  (eq 1) can then be estimated, but it cannot be discerned if  $f(r)$  is influenced by radial motions. As a consequence, exact average internuclear distances cannot be derived from NOE or ROE intensities in the presence of internal motions. However, knowledge of  $\theta^0$  can improve the interpretation of NOE intensities even if a complete description of average distance

(44) Szyperki, T.; Luginbühl, P.; Otting, G.; Güntert, P.; Wüthrich, K. *J. Biomol. NMR* **1993**, *3*, 151–164.

(45) Lee, A. L.; Flynn, P. F.; Wand, A. J. *J. Am. Chem. Soc.* **1999**, *121*, 2891–2902.

(46) Beeser, S. A.; Goldenberg, D. P.; Oas, T. G. *J. Mol. Biol.* **1997**, *269*, 154–164.

(47) Nirmala, N. R.; Wagner, G. *J. Am. Chem. Soc.* **1988**, *110*, 7557–7558.



and radial and angular motion cannot be obtained; in DNA fragments, discrepancies are frequently observed between base–base and sugar–sugar NOE intensities. In the DNA three-way junction 3WJ1,<sup>38</sup> we detected strong internal motions in the sugar moieties, which explained such discrepancies (manuscript in preparation).

Molecular dynamics simulations yield a description of internal motion, from which  $\theta^0$  and NOE rates can be calculated. Agreement of calculated  $\theta^0$  with experimental  $\theta^0$  can serve as a criterion that the molecular dynamics trajectory describes internal motions well.  $\theta^0$  is sensitive to motions on the 100 ps time scale, which can be sampled in nanosecond trajectories. In contrast, calculated NOE rates and experimental NOE rates are hard to compare, because NOE rates are also influenced by slower motions, which are not sampled well in nanosecond trajectories.

The ratio  $R$  is also sensitive to anisotropic tumbling.<sup>18</sup> The orientation of H,H vectors relative to the diffusion tensor of the molecule can, therefore, also influence  $\theta^0$ . In principle, this influence can be used to orient H,H vectors relative to the diffusion tensor, which would be a new source of long-range structural information. However, the variation in  $\theta^0$  caused by anisotropic tumbling is below 1° for all but the smallest molecules (Supporting Information Figure S6). In agreement with this, we did not notice an influence of anisotropic tumbling on  $\theta^0$  for BPTI.

## Conclusions

Internal motions in molecules up to about 15 kDa ( $\omega\tau_c \leq 40$ ) can be detected in off-resonance ROESY experiments as reduction of the zero-crossing angle  $\theta^0$ . The necessary series of off-resonance spectra can be acquired in a reasonable experiment time, and data analysis is straightforward. In our (relatively rigid) model system BPTI, we detected internal motions of the C-terminus, flexible side chains, and methyl

groups. For the flexible side chains, upper limits of the order parameter for side-chain rotation were derived. For many classes of natural products, such as oligosaccharides, isotope labeling is impracticable. Off-resonance ROESY is well suited to study internal motion of unlabeled molecules. Many natural products have a suitable size for off-resonance ROESY, or experimental conditions (temperature, solvent viscosity) can be adjusted so that  $\theta^0$  becomes sensitive to internal motion. For isotope-labeled samples, detection of internal motion by off-resonance ROESY is complementary to heteronuclear relaxation experiments; off-resonance ROESY samples motions about different axes, on different time scales, and can provide information on internal motions of long-range NOEs. The 75 cross-peaks that we analyzed are a small fraction of all cross-peaks that could be analyzed in BPTI. Because there are many more H,H NOEs than X,H bonds in a molecule, there is a wealth of information on internal motion in  $\theta^0$ . Furthermore,  $\theta^0$  directly relates to motions of H,H NOEs which are used in NMR structure calculations. Therefore, structure calculations can be improved, for example, by distinguishing genuinely flexible regions from regions that are ill-defined because of lack of data.

**Acknowledgment.** Parts of this work were presented at the 29<sup>th</sup> AMPERE–13<sup>th</sup> ISMAR, Berlin, August 2–7, 1998, and at the 41<sup>st</sup> ENC, Asilomar, California, April 9–14, 2000. We thank the anonymous reviewers for valuable comments.

**Supporting Information Available:** Four tables of assignments and  $\theta^0$  values for side-chain NOEs and for long-range NOEs. Matlab script for the calculation of  $\theta^0$  from lists of off-resonance ROESY cross-peak integrals. One figure showing the effect of anisotropic tumbling on  $\theta^0$  (PDF). This material is available free of charge via the Internet at <http://pubs.acs.org>.

JA0120400